



Utilization of Heavy Metal Complexes As Phosphorogenic Sensors for the Detection of Amino Acids, (A Review)

ARUMUGAM RAMDASS¹, VEERASAMY SATHISH^{2*} and POUNRAJ THANASEKARAN^{3*}

¹Research Department of Chemistry, Aditanar College of Arts and Science, Tiruchendur - 628 216, India.

²Department of Chemistry, Bannari Amman Institute of Technology, Sathyamangalam - 638 401, India.

³Institute of Chemistry, Academia Sinica, Taipei 115, Taiwan.

Corresponding author E-mail: ptsekarana@yahoo.com, vsathish1985@gmail.com

<http://dx.doi.org/10.13005/ojc/340101>

(Received: December 23, 2017; Accepted: January 12, 2017)

ABSTRACT

The use of phosphorogenic heavy-metal complexes has emerged as an attractive platform for luminescence sensing and cellular imaging studies as a result of several merits including precisely arranging the coordination structures and charge-transfer characteristics. This review intends to provide the design principles and the applications of amino acids sensing based on heavy-metal complexes such as Re(I)-, Ru(II)-, Ir(III)-, and Pt(II). These metal complexes function as phosphorogenic sensors with superior activities and selectivities towards amino acids by utilizing several mechanisms, including luminescent responses of "switch-on". Furthermore, the practical utility of long lifetime and cell permeability of these metal complexes allows to detect luminescence imaging of amino acids in living cells without interference from endogenous fluorophores.

Keywords: Amino acids, Cell imaging, Heavy metal complexes, Phosphorescence, Selectivity.

INTRODUCTION

Amino acids that are bioactive molecules play pivotal roles in maintaining various biological pathways in cellular functions. Especially, biothiols such as cysteine (Cys) homocysteine (Hcys) and reduced glutathione (GSH) are responsible for the

physiological balance in living system¹⁻³. The abnormal levels of these thiols are linked to a number of human diseases, such as cancer, slow growth, edema, liver damage, cardiovascular, Parkinson's disease, Alzheimer's disease, skin lesions, etc^{4,5}. Therefore, typical instrumental detection techniques include colorimetric



detection⁶, electrophoresis⁷, electrochemical assay⁸, high-performance liquid chromatography⁹, Fourier transform infrared (FTIR) spectroscopy¹⁰, mass spectrometry¹¹, and UV-Vis spectrophotometry¹² have been developed and applied for the detection of thiol containing amino acids but they require relatively complicated and multistep reactions, and sophisticated instrumentation.

An alternative technique, fluorescence method exhibits a lot of advantages such as high sensitivity, easy operation, rapid detection, low cost, highly efficient, real-time analysis and easily visualized analysis technique for the detection and quantification of amino acids. Therefore, numerous organic fluorophores have been prepared by modifying their rich chemical structures, and widely used them as probes to detect these amino acids via change in the signal of fluorescence¹³⁻¹⁵. However, most of these fluorophores suffer from low photostability, poor water solubility, interference from background fluorescence, scattered light in real-time applications, short excitation wavelength, and the small Stokes shift. Hence, the development of excellent probes without these drawbacks is highly desired for enabling the wide spread use of sensors that can be applicable to various amino acids.

The introduction of heavy metal ions such as Pt(II)-, Ru(II)-, Re(I)-, Ir(III)- ions into the organic fluorophores was found to be dramatically changed in their emission characteristics. Special features of heavy metal complexes include: high photo-, thermal-, and chemical- stabilities, visible absorption and emission wavelengths, large Stokes shifts, long excited-state lifetimes, signal discrimination from short-lived background fluorescence via spectral and temporal resolution and low cytotoxicity. These excited state properties usually depend on the available metal centers, structure and triplet state of the ligands, and their environments, and associates with intraligand charge-transfer (ILCT), ligand-to-ligand charge-transfer (LLCT), ligand-to metal charge transfer (LMCT), metal-to-ligand charge-transfer (MLCT), metal-metal-to-ligand charge-transfer (MMLCT), ligand-to-metal-metal charge transfer (LMMCT) and metal-to-ligand-ligand charge-transfer (MLLCT) states.

Owing to these outstanding photophysical properties associated with the above transitions, a variety of luminescence probes based on heavy metal complexes have been developed for the detection of amino acids in recent years. Several excellent reviews appeared earlier to focus on this topic as part of their works¹⁶⁻¹⁸. In light of this important field, the aim of this review is to highlight the recent development of heavy metal complexes as sensors for the detection of thiol containing amino acids. The complexation of heavy metal ions with various organic motifs and their photophysical properties will be briefly addressed. Subsequently, the application of these sensors for the detection and imaging of biothiols will be discussed, and their future prospects will be finally outlined.

Phosphorogenic sensing of biothiols by heavy metal complexes

For this purpose, several strategies have been developed over the last decade to sense thiol containing amino acids selectively using phosphorogenic heavy metal complexes such as Re(I), Ru(II), Ir(III), and Pt(II) complexes. The incorporation of thiol-recognition moieties, such as maleimide, aldehyde groups, sulfonate ester, azo linker and disulfide bond into the metal complexes allows to design a variety of thiol responsive luminescent probes. Maleimide containing probes undergo specific coupling with thiols leads to cyclization reaction that would display luminescence responsive behavior. In the case of aldehyde, it readily reacts with cysteine (Cys) or homocysteine (Hcys) to generate thiazinane or thiazolidine moiety, producing the emission signal changes. As arene sulfonate ester or arene sulfonamide is an electron withdrawing group, it quenches the emission intensity of coupled probes via an intramolecular photoinduced electron transfer (PET) process. Upon the cleavage of sulfonate or sulfonamide group by thiols, PET would be inhibited so that the emission of the metal complexes will be switched on. Another strategy is to employ 1,4-addition of thiols to α,β -unsaturated ketones of probes that would disrupt the π -conjugation of metal complex, generating a remarkable enhancement in emission intensity. The introduction of azo linker also quenches the emission intensity of probes via an intramolecular PET process but the luminescence "switching-on"

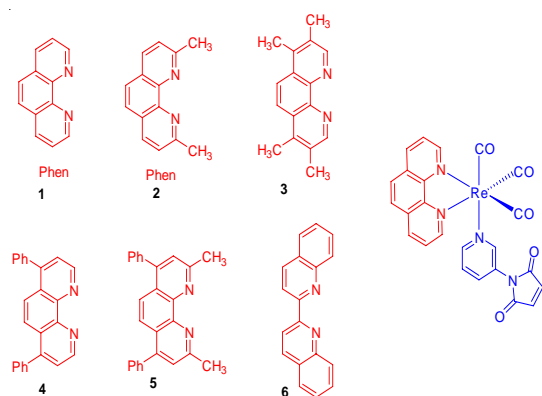
of probes would take place via inhibiting the PET process by the thiol-mediated reduction of azo group.

RESULTS AND DISCUSSION

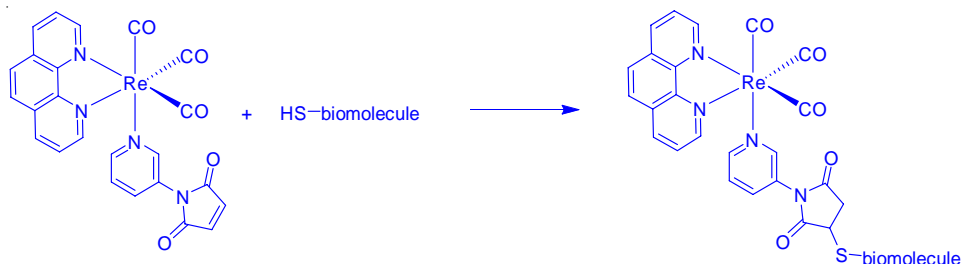
Depending on the nature of the coordinating ligands and metal centers, binding of the thiols at the recognition site would influence their luminescence behaviors to generate the emission signal changes. Some of the recent developments are discussed below.

Re(I) complexes

Using thiol-maleimide bioconjugate reaction strategy, Lo and coworkers prepared a series of maleimide containing rhenium(I) complexes, 1-6 [Re(phen)(CO)₃(py-3mal)](CF₃SO₃) (1), [Re(2,9-Me₂-phen)(CO)₃(py-3mal)](CF₃SO₃) (2), [Re(3,4,7,8-Me₄-phen)(CO)₃(py-3mal)](CF₃SO₃) (3), [Re(4,7-Ph₂-phen)(CO)₃(py-3mal)](CF₃SO₃) (4), [Re(2,9-Me₂-4,7-Ph₂-phen)(CO)₃(py-3mal)](CF₃SO₃) (5), and [Re(biq)(CO)₃(py-3mal)](CF₃SO₃) (6) (Scheme 1)¹⁹. The chemical composition of these complexes was analyzed by NMR, positive-ion ESI-MS, IR and elemental analyses.



Scheme 1. Chemical structure of Re(I) complexes 1-6

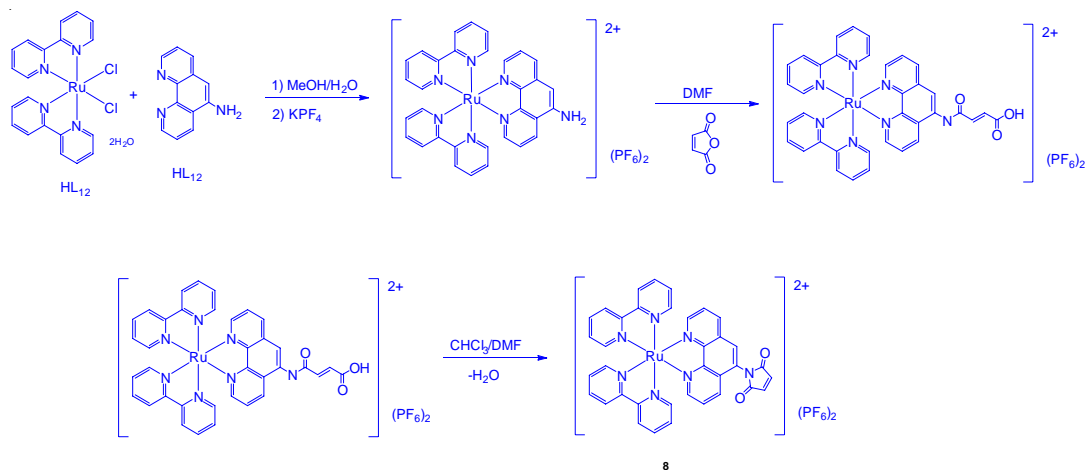


Scheme 2. Proposed reaction between the complex cation of 1 and the sulfhydryl group of a biomolecule

UV-Vis absorption spectra of 1-3 in CH₂Cl₂ showed intense absorption bands at 250-296 nm and a shoulder at 324-364 nm that are assigned to intraligand (IL) and metal-to-ligand charge-transfer (¹MLCT) transitions, respectively. On the other hand, complexes 4-6 showed these transitions at 332-382 and 374-408 nm, respectively, because of increasing π-conjugation effect of coordinated ligands. Upon excitation at > 350 nm, these complexes emitted ³MLCT at 514-632 nm in CH₂Cl₂ with a lifetime of 0.10 to 7.42 ms. Utilization of these complexes as site-specific labels for biological sulfhydryl species led to generate long-lived ³MLCT emissions. For example, thiolated M13 sequencing primer M13-R [5'-HS(CH₂)₆-AACAGCTATGACCATG-3'], glutathione (GSH), bovine serum albumin (BSA) and human serum albumin (HSA) labeled with 1 showed a typical ³MLCT [*d*p(Re) → π*(phen)] character. The emission of the bioconjugate 1-GSH was efficiently quenched by oxygen whereas the complex 1 coupled to BSA, and HSA was shielded in the interior away from surrounding exposure, and hence, their emission were less quenched. The authors designed maleimide containing complex 1 to react with sulfhydryl biomolecules specifically and generate its thioether derivative (Scheme 2). In another study, a modified rhenium(I) complex [Re(bpy)(CO)₃(py-CH₂Cl)]⁺ (7) was used to assess intracellular mitochondria of human breast adenocarcinoma cells²⁰.

Ruthenium(II) complexes

Following a similar mechanism, a thiol-reactive Ru(II) complex containing a maleimide group, bis(2,2'-bipyridine) (5-maleimide-1,10-phenanthroline) ruthenium (II) di(hexafluorophosphate) (8) was prepared (Scheme 3)²¹.

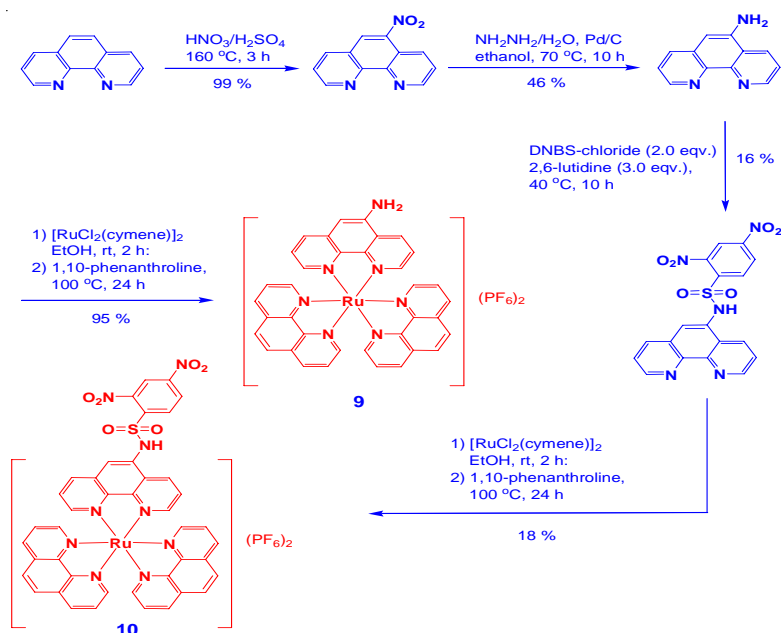


Scheme 3. Synthetic pathway for the thiol-reactive complex 8 starting from commercially available reagents

Complex 8 showed a MLCT absorption band at 454 nm, and gave an emission at 606 nm with a quantum yield of 3.6%. Emission analysis of 8 revealed that a significant emission was observed upon thiol conjugation. Furthermore, the labelling of HSA to 8 in combination with an acceptor cyanine dye and antibody permitted to study the influence of antibodies in a LET immunoassay at the nanomolar level.

One of the strategies to generate thiol-selective luminescent metal complexes is

based on the cleavage of electron sink 2,4-dinitrobenzenesulfonyl motif (DNBS), which shows emission OFF-ON switching with good selectivity, from metal complexes in the presence of thiols. This process significantly results in phosphorescence enhancement. In 2010, Zhao group prepared two ruthenium(II) complexes $[(1,10\text{-phenanthroline})_2\text{ruthenium}(5\text{-amino-}1,10\text{-phenanthroline})]^{2+}(\text{PF}_6^-)_2$ (9) and $[(1,10\text{-phenanthroline})_2\text{ruthenium}(5\text{-(2,4-dinitrobenzenesulfonylamide)-}1,10\text{-phenanthroline})]^{2+}(\text{PF}_6^-)_2$ (10) as shown in Scheme 4.²²



Scheme 4. Syntheses of complexes 9 and 10

UV-Vis absorption spectra of compounds 9 and 10 showed a pi-pi ligand centered transition below at 300 nm and a MLCT band at 400-500 nm. Upon excitation, complex 9 showed a ³MLCT red emission at 600 nm with a long lifetime of is where as complex 10 displayed no emission owing to the quenching of MLCT band via the photoinduced electron transfer (PET) from electron rich Ru center to electron deficient DNBS moiety. In the presence

of thiols, cleavage of DNBS induced the increase in the emission intensity of 10, as high as 90-fold. Furthermore, compound 10 showed only a selective sensing towards thiol groups. The sensing mechanism of 10 with thiols was proposed and supported by DFT calculations. Cellular studies revealed that upon excitation compound 10, showing red emission, was specific towards intracellular thiols among other analytes (Fig. 1). The authors believed that this work was the first report, showing the emission OFF-ON switch effect for the selective detection of thiol using ruthenium complex.

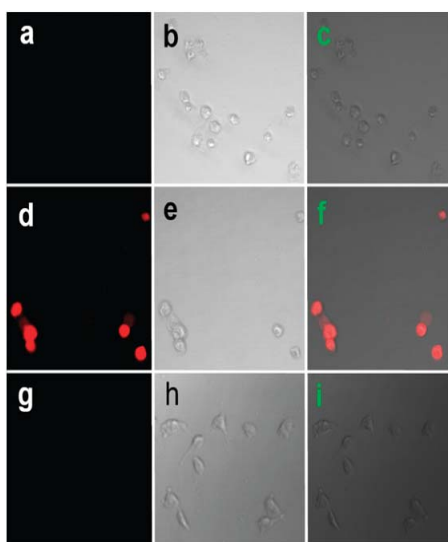
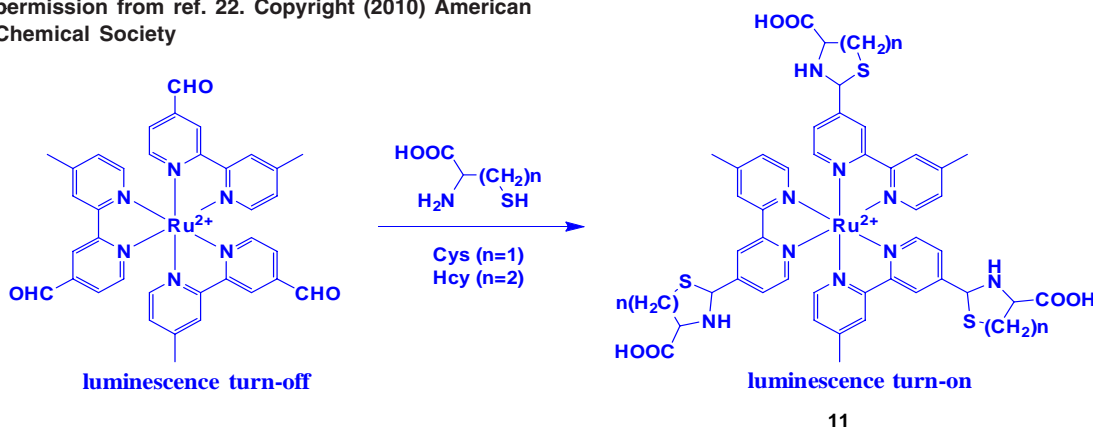


Fig. 1. Luminescence images of NCI-H446 cells. (a) Images of cell. (d) Images of cells incubated with probe 10 (30 μ M) for 8 h at 37 $^{\circ}$ C. (g) Images of cells pretreated with *N*-methylmaleimide (0.5 mM) for 1 h at 37 $^{\circ}$ C and then incubated with probe 10 (30 μ M) for 8 h at 37 $^{\circ}$ C. (b, e, h) Bright field images corresponding to images a, d, g. (c) Overlay of images a and b. (f) Overlay of images d and e. (i) Overlay of images g and h. Reproduced with permission from ref. 22. Copyright (2010) American Chemical Society

Ruthenium(II) complexes display outstanding photochemical and photophysical properties have been utilized as luminescence probes for the specific detection of biomolecules. In 2010, Yuan and coworkers prepared a tris(4-methyl-2,2'-bipyridyl-4'-carboxaldehyde) ruthenium(II) hexafluorophosphate, [Ru(CHO-bpy)₃] (PF₆)₂ (11) complex by refluxing a mixture of CHO-bpy and RuCl₃·3H₂O in EtOH/H₂O under inert atmosphere and employed as a probe for sensing of cysteine (Cys) and homocysteine (Hcys) (Scheme 5)²³.

UV-Vis spectrum of 11 displayed two strong absorption bands at 300 and 485 nm, which are attributed to the ligand localized π - π^* and metal-to-ligand charge transfer (MLCT) transitions, respectively. Interestingly, addition of Cys and Hcys into a solution of 11 induced a blue-shifted absorption response of 11 from 485 to 465 nm and 300 to 290 nm with a color change from orange to yellow. In this methodology, compound 11



Scheme 5. Luminescence response reaction of 11 towards Cys/Hcys

contained aldehyde groups that function not only to quench the luminescence behavior of 11, and hence it is non-emissive, but also recognize specific amino acids. Addition of Cys and Hcys resulted in significant luminescence enhancement and a blue-shifted emission from 720 to 635 nm with a detection limits of 1.41 and 1.19 mM, respectively (Fig. 2). Based on the absorption and emission studies, it

can be attributed by the formation of corresponding thiazolidine and thiazinane derivatives because of the degradation of aldehyde groups in 11. Furthermore, this compound was highly selective for Cys/Hcys over other biomolecules such as other amino acids, DNA and proteins. This result suggests that luminescence change of 11 depends on the nature of the binding interaction between the aldehyde groups and the Cys/Hcys motifs (Scheme 5).

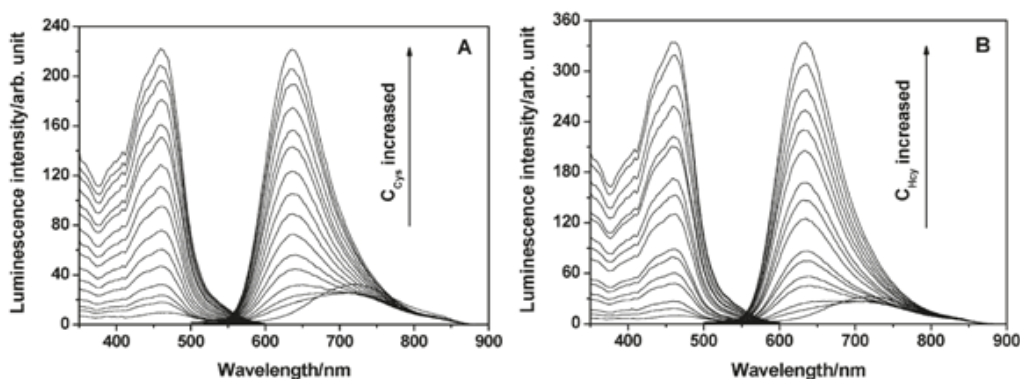


Fig. 2. Excitation and emission spectra of 11 (10 μ M) in the presence of different concentrations of Cys (A) and Hcys (B). The concentrations of Cys and Hcys are 50, 100, 150, 200, 250, 300, 400, 500, 600, 750, 900, 1200, 1500, 2100, and 3000 μ M, respectively. Reproduced with permission from ref. 23. Copyright (2010) American Chemical Society

In another work using the similar strategy, a series of ruthenium(II) complexes (12-15) containing mono- or di-substituted aldehyde groups in one of the bpy ligands have been synthesized for the selective recognition of Hcys and Cys²⁴. Compounds 12-15 (Fig. 3) were prepared by

refluxing the reaction mixture of cis-Ru(bpy)₂Cl₂·xH₂O or cis-Ru(dmb)₂Cl₂·xH₂O and 4-methyl-2,2-bipyridine-4-carboxaldehyde (L1) and 4,4-diformyl-2,2-bipyridine (L2) in ethanol under N₂ atmosphere. These compounds were characterized by NMR, MS-FAB and elemental analyses.

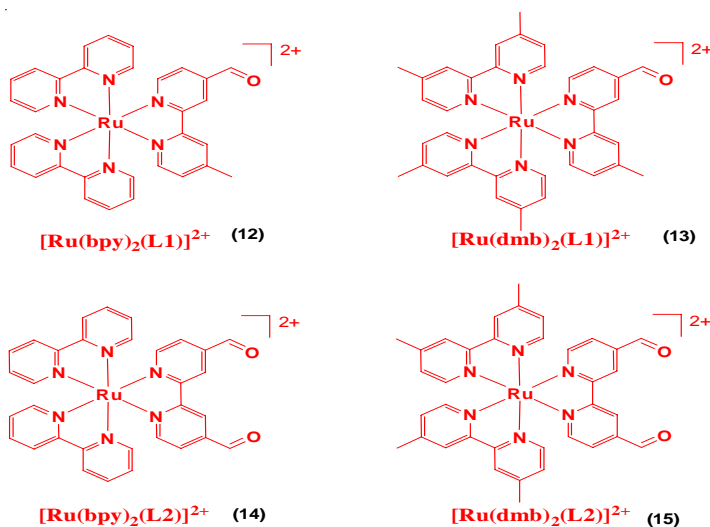
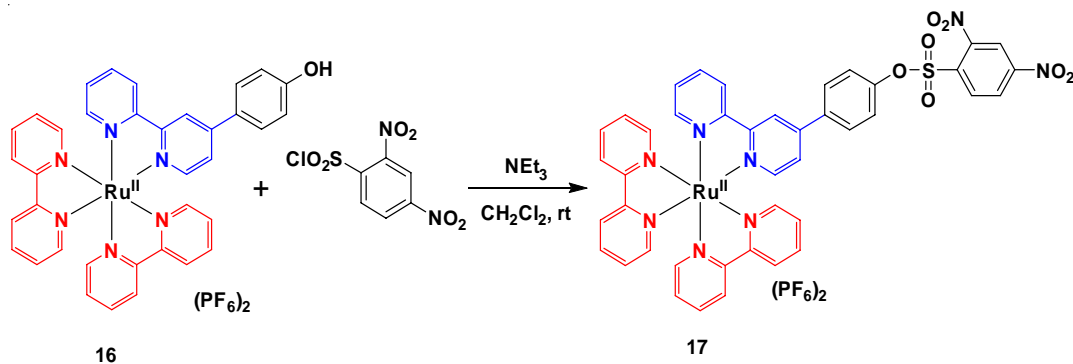


Fig. 3. Structures of the synthesized ruthenium(II) complexes 12-15

The electronic absorption spectra of 12-15 exhibited an intense high-energy absorption bands at 276-308 nm, and a weak low-energy bands at 416-492 nm, corresponding to their intraligand (IL) and metal-to-ligand charge transfer (MLCT, $d\pi(\text{Ru}) \rightarrow \pi^*(\text{ligand})$) transitions, respectively. These complexes showed a weak triplet MLCT emission at 605-617 nm at room temperature because electron-withdrawing aldehyde groups quenched the MLCT emission of 12-15. Upon the addition of Hcys, the intensity of 15 at 492 nm decreased followed by the appearance of a new band at 461 nm with a blue-shift of 31 nm and two isosbestic points at 431 and 482 nm. Other absorption bands displayed a smaller or no changes with isosbestic points at 304, 328 and 366 nm. This result demonstrated that more aldehyde groups present in metal complexes would provide a larger spectral changes while interacting with Hcys or Cys, indicating their key role in the specific recognition studies. Addition of Hcys to compounds 12 and 13 caused a remarkable increase in luminescence intensity by 1.6- and 1.9-fold with the detection limit of 4 and 15 mM, respectively, while a maximum increase of 8.5- and 10.1-fold with the detection limit of 2 and 13 mM, respectively, in the emission enhancement of the 14 and 15 was

registered. On the other hand, a maximum of 1.3-, 3.5-, 1.6- and 4.5-fold with the detection limit of 5, 2, 4 and 1 mM, respectively, emission enhancement of 12-15 was recorded at saturation in the presence of Cys. Compared with 12 and 13, compounds 14 and 15 showed a high affinity towards Cys and Hcys because of the presence of two aldehyde groups, giving a strong enhancement of the emission intensity. This is presumably due to the formation of thiazinane. Therefore, compounds 12-15 were highly selective for Cys and Hcys over other amino acids as only Cys and Hcys could induce luminescence enhancement of these complexes.

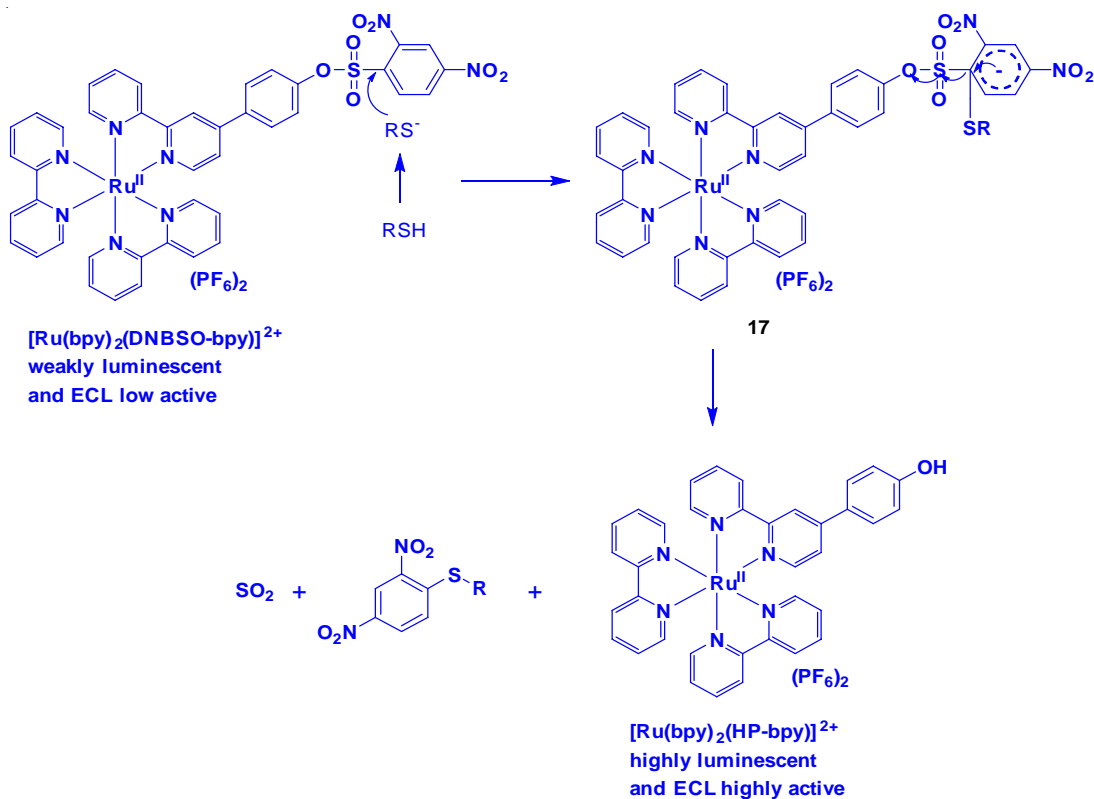
Owing to the excellent photophysical properties of Ru(II) complexes, Yuan and coworkers²⁵ prepared a Ru(II) complex, $[\text{Ru}(\text{bpy})_2(\text{DNBSO-bpy})](\text{PF}_6)_2$ (bpy = 2,2'-bipyridine; DNBSO-bpy = 2,4-dinitrobenzenesulfonate of 4-(4-hydroxyphenyl)-2,2'-bipyridine), (17) by the treatment of $[\text{Ru}(\text{bpy})_2(\text{HP-bpy})](\text{PF}_6)_2$ (16)²⁶ with 2,4-dinitrobenzenesulfonyl chloride in dry CH_2Cl_2 in the presence of NEt_3 at room temperature (Scheme 6) and used these two complexes 16 and 17 for the sensing of thiol containing amino acids by photoluminescence (PL) and electrochemiluminescence (ECL) detection techniques.



Scheme 6. Synthesis of Ru(II) complex 17 from 16

Complexes 16 and 17 displayed a MLCT band at 456 nm in HEPES buffer solution (pH = 7.0). Treatment of 16 with 2,4-dinitrophenol did not show any observable changes in the luminescence spectrum of 16. However, addition of thiol into 17 led to generation of quenching process, confirming that the intramolecular PET took place. Complex 17 showed a weak emission at 612 nm, whereas complex 16 displayed a highly

emission at 612 nm by 23-fold to that of 17. Upon the incremental addition of Cys or GSH, the excitation and emission intensity of 17 enormously increased with the detection limit of 20.1 and 19.8 nM, respectively, in a 1:1 binding stoichiometry. However, other amino acids did not trigger any changes in the emission of spectrum of 17. These results demonstrated that compound 17 is highly selective for the detection of thiol amino acids (Scheme 7).



Scheme 7. Response reaction of 17 toward thiols

As evidenced by PL technique, the ECL intensity of 17 was also enormously increased with the detection limit of 86.5 and 56.3 nM, respectively, after the addition of Cys and GSH. At the same time, other amino acids and metal cations did not show any response towards the ECL intensity of 17. Complex 17 treated HeLa cells displayed a red emission in the cytosol, indicating that this complex penetrated into the membrane and reacted with intracellular thiol. In the presence thiol scavenger N-ethylmaleimide, no luminescence from complex

17 treated HeLa cells was found. However, when GSH was incubated with these non-luminescent cells, a strong red emission appeared from the cells, indicating the reaction of complex 17 with intracellular thiol groups. It was too difficult to detect imaging study by ECL technique because complex 17 reacted with thiols at the electrode surface.

Ji and coworkers prepared an azo containing Ru(II) complex (18, Fig. 4) by heating the reaction mixture of Ru(bpy)₂Cl₂ and azobpy ligand in EtOH/H₂O mixture²⁷.

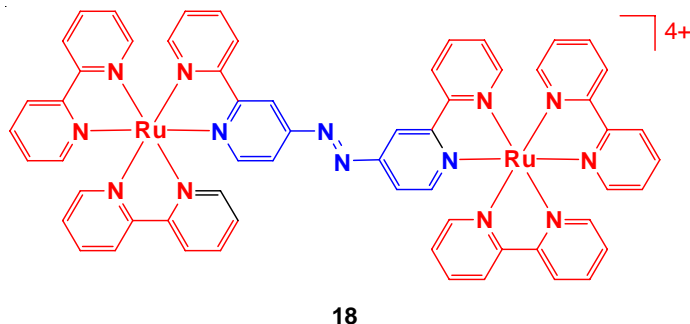
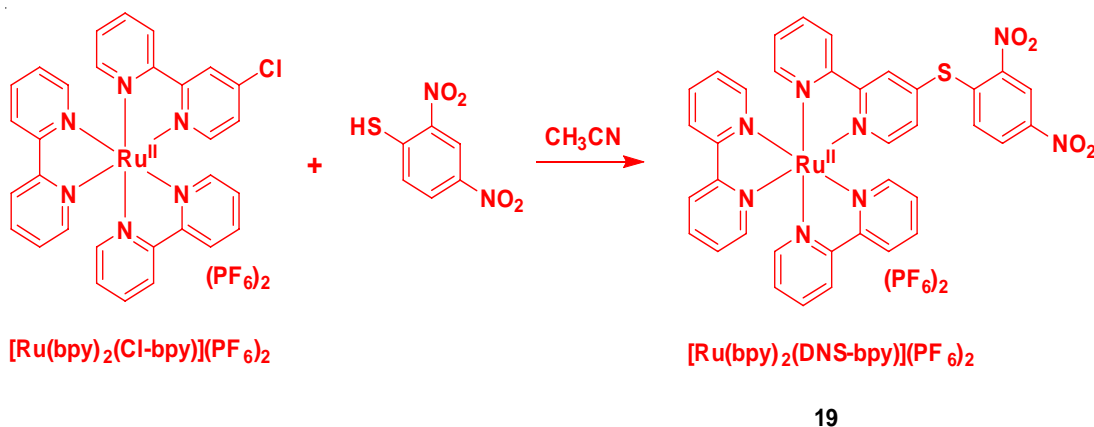


Fig. 4. Chemical structure of complex

Addition of Cys, Hcys and GSH into the complex 18 resulted in the decrease of absorption intensity at 562 nm (MLCT ($\pi \rightarrow$ azobpy π^*) with a hyperchromic effect followed by increase of absorbance at 439 nm along with red shifted (attributed to MLCT ($\pi \rightarrow$ bpy π^*) in a 2:1 stoichiometry ratio. During this reaction, the color of the solution from gray to yellow was appeared. This complex showed a weak emission at 605 nm because of quenching by azo linker via an intramolecular PET process. Upon the reduction of azo group by thiols, PET is inhibited so that the emission of the complex is switched on. Addition of Cys, Hcys and GSH enhanced the intensity of 18 by 35-, 36-, and 33-fold with the detection limit of 2.29×10^{-7} , 2.27×10^{-7} , and 2.42×10^{-7} M, in a 2:1 binding ratio, respectively. However, other amino acids including Cystine (oxidative form of Cys linked by disulfide) did not show any observable changes

in the absorption and emission spectra of 18. Under UV light, thiols can be differentiated from other amino acids by showing red color in the presence of 18. This results indicated that complex 18 is selectively sensing thiol amino acids.

In another study, Yuan *et al.*, designed a non-emissive complex that can be restored its emissive property upon interaction with thiol. Compound, $[\text{Ru}(\text{bpy})_2(\text{DNS-bpy})](\text{PF}_6)_2$ [bpy = 2,2'-bipyridine, DNS-bpy = 4-(2,4-dinitrophenylthio)-2,2'-bipyridine] (19) was obtained by heating the reaction mixture of $[\text{Ru}(\text{bpy})_2(\text{Cl-bpy})](\text{PF}_6)_2$ (bpy = 2,2'-bipyridine, Cl-bpy = 4-chloro-2,2'-bipyridine) and 2,4-dinitrothiophenol in the presence of K_2CO_3 and KI in anhydrous CH_3CN under inert atmosphere (Scheme 8)²⁸. This compound was characterized by NMR, MS, and elemental analyses.



Scheme 8. Reaction pathway for the synthesis of Ru(II) compound, 19

Absorption spectrum of 19 in the absence and presence of GSH, Cys or Hcys in ethanol-HEPES buffer (pH 7.2) showed only a typical MLCT band (458 nm). However, a significant enhancement at 330 nm in 19 was observed along with the formation of new absorption band related to 2,4-dinitrophenyl moiety, after the addition of GSH, Cys and Hcys. This result demonstrated that thiols cleaved 2,4-dinitrophenyl moiety from the complex 19, which is in agreement with the previous report²⁶. In the absence of biothiols, complex 19 displayed a weak emission at 625 nm upon excitation at 458 nm. Investigation of luminescence

response of 19 towards biothiols showed that GSH cleaved DNBS moiety and induced the increase in the emission intensity of 19, as high as 80-fold with the detection limit of 1.0 μM , indicating its highly sensitive detection of biothiols (Fig. 5). In addition, the effect of pH on the emission response of 19 towards biothiols was also examined.

The electron withdrawing 2,4-dinitrophenyl moiety quenched the emission of 19. However, thiols underwent $\text{S}_\text{N}\text{Ar}$ substitution reaction and cleaved to eliminate 2,4-dinitrophenyl moiety from 19, so that the MLCT emission of 19 can be restored (Scheme 9).

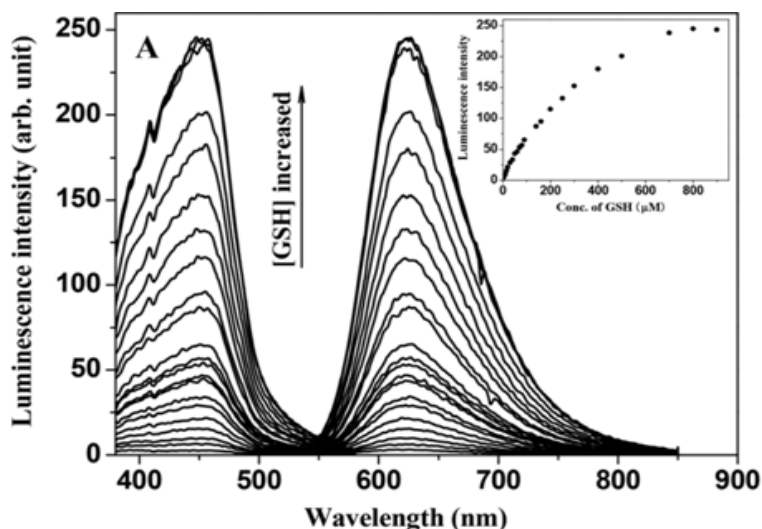
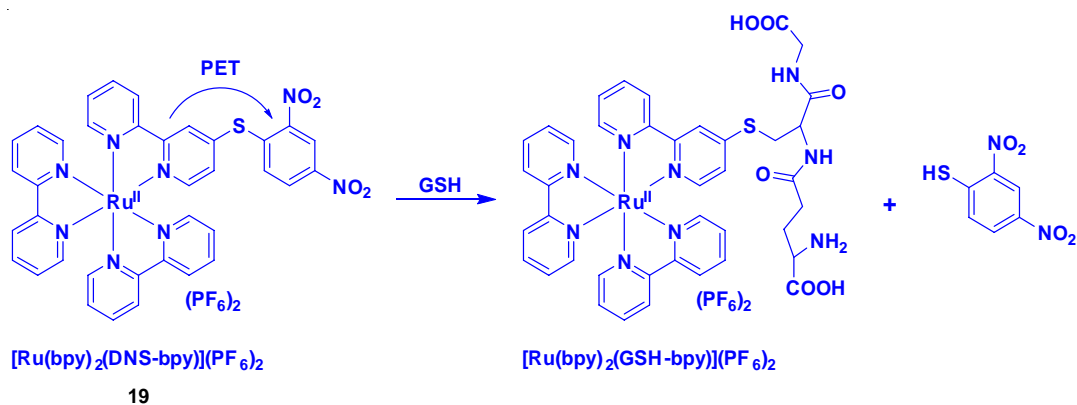


Fig. 5. Excitation and emission spectra of 19 (10 μM) in the presence of different concentrations of GSH (0, 5, 10, 15, 20, 30, 40, 50, 60, 70, 80, 90, 140, 160, 200, 250, 300, 400, 500, 700, 800, 900 μM) in 1:4 ethanol-50 mM HEPES buffer of pH 7.2 at room temperature (the inset shows the emission intensity changes at 625 nm in the presence of different concentrations of GSH). Reproduced with permission from ref. 28. Copyright (2014)

Royal Society of Chemistry



Scheme 9. Structure of 19 and its luminescence response following reaction with GSH

Compared with GSH, both Cys and Hcys triggered a much lower luminescence enhancement in 19 because they attacked the carbon attached to the sulfur to form stable C-N bond. But GSH has no adjacent amino group, which is very difficult to lead intramolecular substitution. At the same time, other amino acids could not be able to induce the emission intensity of 19. Lastly, the emission imaging of biothiols in *Daphnia magna* animal study using compound 19 demonstrated its applicability towards biothiols specifically.

Iridium(III) complexes

In order to demonstrate the utility of metal complexes in protein staining, two cyclometalated iridium complexes, $[\text{Ir}(\text{ppy})_2(\text{solv})_2]^+$ (20; ppy = 2-phenylpyridine; solv = H_2O or CH_3CN) and $[\text{Ir}(\text{ppy})_3]$ (21) were chosen (Fig. 6). Treatment of $[\text{Ir}(\text{ppy})_2\text{Cl}]_2$ with AgOTf in the presence of H_2O or CH_3CN resulted in the formation of complex 20 whereas compound 21 is formed by dissolving the dimer $[\text{Ir}(\text{ppy})_2\text{Cl}]_2$ in 1M HCl²⁹.

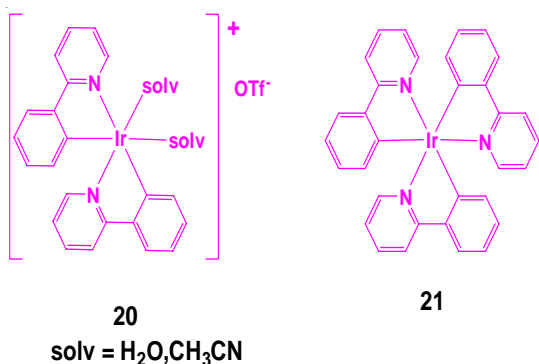


Fig. 6. Structure of cyclometalated iridium complexes 20 and 21

Complex 20 showed a weak emission in phosphate buffered saline (PBS). However, the addition of histidine (His) induced the emission

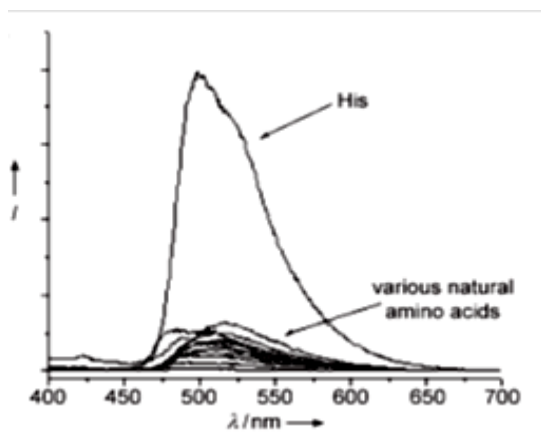
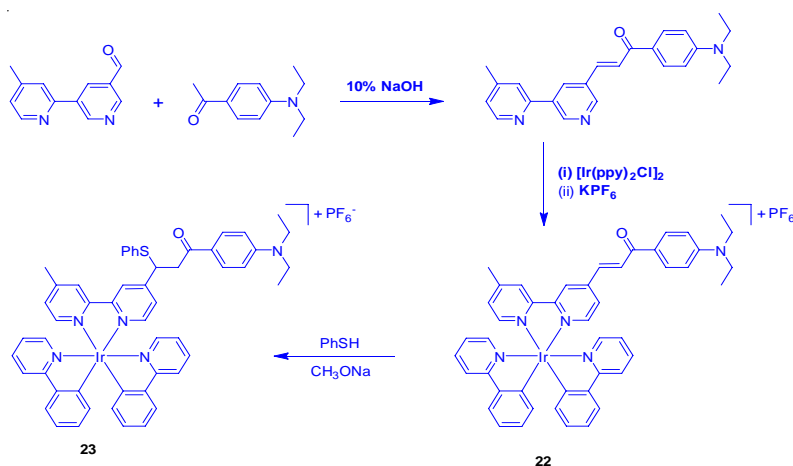


Fig. 7. Emission spectra of 20 (50 μM) in PBS buffer with His and various natural amino acids (200 μM) at 20 °C. Reproduced with permission from ref. 29. Copyright (2008) John Wiley & Sons

enhancement of 20. On the other hand, other amino acids responded with weak or no emission (Fig. 7). This result suggested that compound 20 was selectively sensing His, which was also confirmed by electrospray-ionization positive-ion mass spectrometry.

High abundance of histidine residues, such as bovine serum albumin (BSA) also induced the emission enhancement of 20. In contrast, compound 21 did not show any response in its emission intensity with BSA. Furthermore, the response of 20 to BSA was not affected by non-protein substances such as inorganic salts, chelating agent EDTA, and detergents like SDS, Triton X-100. As this complex 20 recognized histidine and histidine-rich proteins, it can be applied to the detection of proteins through Western blot and SDS-PAGE gel analyses.

By inspiring the strategy of 1,4-addition of thiols to α,β -unsaturated ketones, Chen and coworkers³⁰ designed cyclometalated iridium(III) complex [Ir(ppy)₂(L)](PF₆)₂ (22), which was obtained by the treatment of functionalized 2,2'-bipyridine with Ir₂(ppy)₄(μ -Cl)₂ precursor in CH₂Cl₂-CH₃OH mixture under reflux (Scheme 10), and studied the conversion of ³ILCT to a mixed ³MLCT and ³LLCT state upon thiol detection. The 1,4-additive reaction of 22 with benzenethiol resulted in the formation of compound 23. These compounds were characterized by positive ion ESI-MS, NMR, elemental analyses, and X-ray crystallographic studies.



Scheme 10. Synthetic routes to 22 and 23

Complex 22 displayed an ppy-, and functionalized bpy-based transition at 280-320 nm, and intraligand charge transfer (ILCT) transition mixed with $[5d(Ir) \rightarrow \pi^*(L)]$ MLCT and $[\pi(ppy) \rightarrow \pi^*(L)]$ LLCT transition at 450 nm, which was supported by DFT calculations. Addition of Cys into a DMF-HEPES buffer solution of 22 showed a decrease in the intensity at 450 nm followed by increase in the intensity at 350 nm with the isosbestic points at 325 nm and 372 nm, indicating the formation of new species. Compound 22 showed a broad emission at 587 nm with a quantum yield of 0.013 and a lifetime of 109 ns, which was originated from 3 ILCT mixed with 3 LLCT and 3 MLCT states. The 3 ILCT excited state deactivated effectively non-radiative process, and hence compound 22 was weakly emissive. Upon the addition of 80 equiv. of Cys or Hcys, the emission intensity of 22 at 587 nm showed a 20-, and 14-fold enhancement with increasing their lifetime of 358 and 127 ns, respectively (Fig. 8). Based on the observations from UV-Vis and emission studies, it was clear that the thioether moiety in the adduct 22-Cys/22-Hcys converted the emission from 3 ILCT excited state to a highly emissive $^3[\pi(ppy) \rightarrow \pi^*(L)]$ 3 LLCT and $^3[5d(Ir) \rightarrow \pi^*(L)]$ 3 MLCT states. Compound 23 showed an intense emission band at 587 nm with a lifetime of 131 ns. The reactivity of 22 towards thiols was found in the order of Cys>Hcy>GSH, indicating the importance

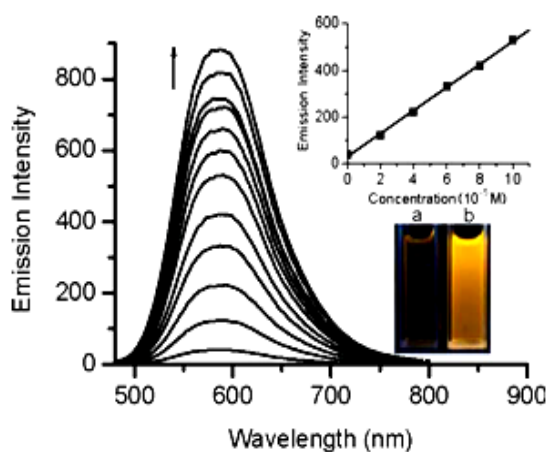
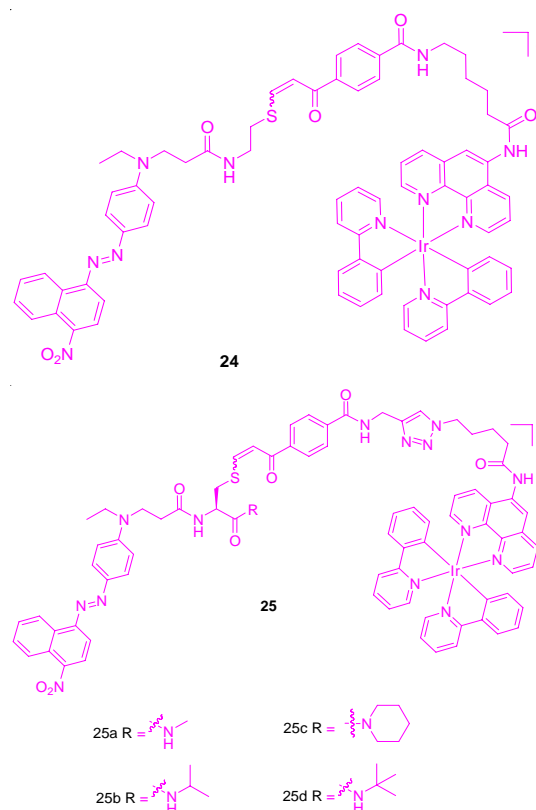


Fig. 8. Changes in emission spectra of complex 22 (20 mM) in DMF-HEPES buffer solution (50 mM, pH 7.2, 4:1, v/v) upon titration with Cys (0–80 equiv). The equilibration time is *ca.* 40 min. Top inset: Plot of the emission intensity at 587 nm as a function of Cys concentration (0– 10^{-4} M). Bottom inset: Luminescence images before (a) and after (b) addition of 80 equiv Cys. Reproduced with permission from ref. 30. Copyright (2010) Royal Society of Chemistry

of steric hindrance effect. The UV-vis and emission responses of 22 towards competitive amino acids showed no significant changes in their spectra except Cys. This result demonstrated that the sensing properties of 22 to Cys was selective, which was also confirmed by ESI-MS and NMR measurements. Furthermore, DFT studies supported a remarkable intensity enhancement by the conversion of ILCT transition in 22 to the MLCT/LLCT states in 22-Cys when Cys interacted with a,b-unsaturated ketone in 22.

Previously, Li and co-workers found a long response time for detecting cysteine (Cys) and homocysteine (Hcy) using two iridium(III) complexes, $[Ir(pba)_2(acac)]$ and $[Ir(pba)_2(bpy)]^+$ ($pba = 4$ -(2-pyridyl)benzaldehyde, $acac =$ acetylacetonate, and $bpy = 2,2'$ -bipyridine)^{31,32}. But, Che group developed a series of iridium(III) complexes (24 and 25a-25d) derivatized with a diarylazo quencher based on fluorescence resonance energy transfer (FRET) strategy (Scheme 11) that exhibits a short response time for sensing of these thiol containing amino acids³³.



Scheme 11. Chemical structure of compounds 24 and 25a-25d

Compound 24 was exhibited to be weakly emissive as the azo dye quenched the luminescence signal of Ir(III) chromophore. But, a maximal 46-fold emission enhancement of 24 at 590 nm was observed with the detection limit of 0.13 mM in response to Hcy under optimal condition, while the emission of 24 was enhanced by 33-fold in the presence of Cys. The increase in emission of 24 was attributed by the nucleophilic attack of Cys or Hcys at the vinyl sulfide linkage of 24 to displace azo quencher from the metal complex. Furthermore, this complex displayed significant selectivity for Cys,

and Hcy over a panel of other amino acids including GSH (Fig. 9). As alkyl R group in compound 25 enhanced steric clouds around vinyl sulfide linkage, the smaller Hcys can easily cleave the azo dye from the Ir(III) chromophore, thus restoring the emission intensity of 25. Due to bulky nature of thiol-containing GSH, it was not able to hinder the nucleophilic attack against the vinyl sulfide linkage of 25, and therefore, its response almost was lacking. Among the probes 24 and 25a-25d, the *tert*-butyl group in 25d was able to distinguish between Hcys and Cys with a selectivity ratio of 5:1.

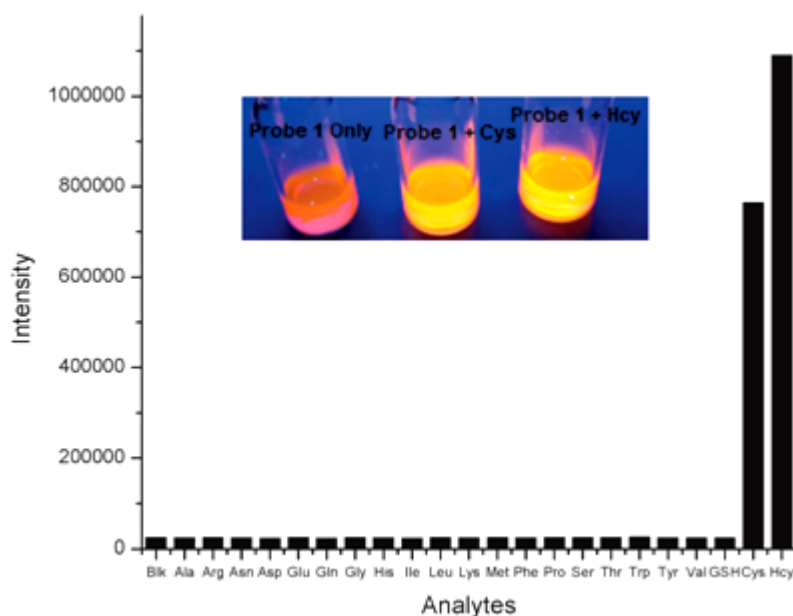
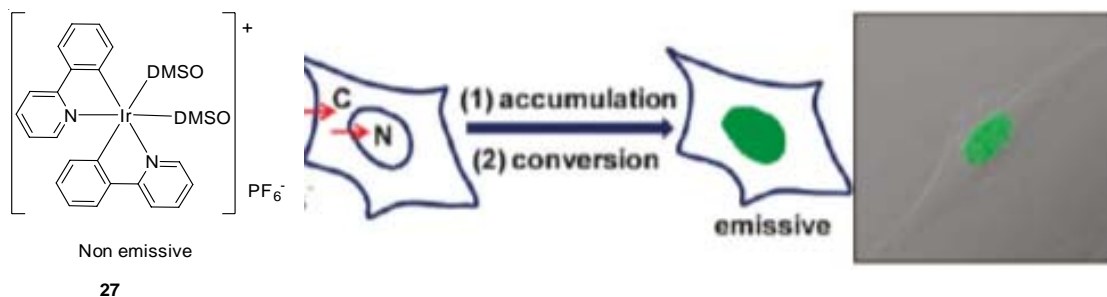


Fig. 9. Emission enhancement in the detection of different analytes by 24. Reproduced with permission from ref. 33. Copyright (2013) Royal Society of Chemistry

In another study, Huang and coworkers³⁴ demonstrated that quaternary amino group attached to the phenanthroline ligand in cyclometallated iridium(III) complexes $[\text{Ir}(\text{C}^{\wedge}\text{N})_2\text{pto}]^+\text{PF}_6^-$ (26a-26d, $\text{C}^{\wedge}\text{N}$ = 2-(2,4-difluorophenyl)pyridine (dfppy), 2-(4-(*tert*-butyl)phenyl)pyridine (*t*-buppy), 2-(thiophen-2-yl)quinoline (thq), 4-(pyridin-2-yl)benzaldehyde (pba) and pto = the quaternization of the tertiary amino group containing 2-chloro-N-(1,10-phenanthrolin-5-yl)acetamide (cpa) ligand) showed a good water solubility and functioned as sensors for the selective detection of Cys and Hcys in an intracellular environment.

Li and coworkers³⁵ firstly demonstrated a new strategy for detecting the nuclei of living

cells using non-emissive iridium complex as a reaction-based light-up imaging agent (Scheme 12). The cyclometalated iridium(III) solvent complex, $[\text{Ir}(\text{ppy})_2(\text{DMSO})_2]^+\text{PF}_6^-$ (27), was prepared by heating the reaction mixture of $[(\text{ppy})_2\text{Ir}(\mu\text{-Cl})_2\text{Ir}(\text{ppy})_2]$, which was obtained upon the reaction of $\text{IrCl}_3 \cdot 3\text{H}_2\text{O}$ with 2-phenylpyridine (ppy) under reflux, and DMSO solvent. UV-Vis absorption spectrum of 27 in HEPES buffer solution exhibited an intraligand ($\pi\text{-}\pi^*$) ppy transition at 250-325 nm, and a mixed singlet and triplet metal-to-ligand charge-transfer ($^1\text{MLCT}$ and $^3\text{MLCT}$) transition as a weak band at 330-470 nm. Compound 27 is non-luminescent both in solution and solid states.



Scheme 12. Chemical structure and the proposed mechanism of nuclear staining with nonemissive iridium(III) complex **27**. The characters 'C' and 'N' denote cytoplasm and nucleus, respectively. Reproduced with permission from ref. 35. Copyright (2011) American Chemical Society.

Cellular uptake studies of non-emissive compound **27** showed a bright emission in the region of nuclei upon incubating with HeLa, KB, FLS, and MSC cells under excitation at 488 nm. In addition, its emission was perfectly colocalized with the nuclear counterstain Hoechst 33258, indicating the characteristic of its imaging probe without the assistance of any membrane-permeable agent (Fig. 10). It was also found that complex **27** possessed a low toxic effect towards cellular nuclei.

The luminescence signal of **27** is enormously induced at different enhancements when it interacted with histidine and histidine-rich proteins. It is proposed that this complex **27** was able to permeate the membranes of living cells via energy-dependent entry pathway and convert into emissive adduct after accumulating the nuclei of living cells (Scheme 12). This complex showed

several advantages include short duration for cell staining, excitation using visible light, high signal ratio between the cytoplasm and the nucleus, low cytotoxicity, and no conjugation required in association with a cell-penetrating molecular transporter, to light up nuclear staining of living cells in biomedical research.

Due to the advantageous photophysical properties of iridium(III) complex, Huang *et al.*,³⁶ prepared probe **29** by the reaction of Ir (III) complex **28**, which was obtained through complexation of $[\text{Ir}(\text{C}^{\wedge}\text{N})_2\text{Cl}]_2$ ($\text{C}^{\wedge}\text{N}$ = 2-(thiophen-2-yl)quinoline) with 3-hydroxypicolinic acid, and 2,4-dinitrobenzene-1-sulfonyl chloride as shown in Scheme 13. Its chemical structure was confirmed by NMR and MALDI-TOF mass spectroscopies.

Complex **29** showed two intense absorption bands at 289 and 335 nm and a moderate band at 400-500 nm that are corresponding to ligand-centered and mixed singlet and triplet metal-to-ligand charge-transfer in associated with ligand-to-ligand charge-transfer transitions, respectively. As DNBS moiety quenched the emission of **29** via PET pathway, probe **29** was non-emissive, which was demonstrated clearly by DFT calculation. Treatment of Cys with probe **29** resulted in the increase in absorbance of **29** at 250-550 nm, showing the interaction of Cys towards probe **29**. In the case of emission properties of **29**, upon the addition of Cys, a significant emission is observed at 603 nm, which is similar to that of emission band of compound **28**. The "OFF-ON" luminescence sensing mechanism was proposed by the fact that cleavage of sulfonate ester of probe **29** by Cys afforded red light emitted complex **28**, which was clearly demonstrated by ¹H NMR,

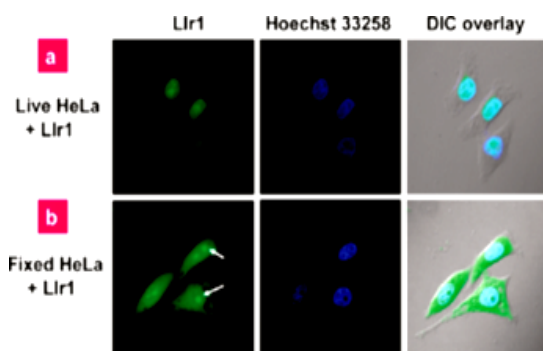


Fig. 10. Confocal luminescence images of (a) living HeLa cells incubated with 10 μM **27** in DMSO/PBS (pH 7.4, 1:99, v/v) for 10 min at 37 °C and then further incubated with Hoechst 33258, and (b) fixed HeLa cells stained with **27** and Hoechst 33258 under the same conditions. Arrows point to the nucleolus of HeLa cells. Reproduced with permission from ref. 35. Copyright (2011) American Chemical Society

time-resolved and MALDI-TOF mass spectral techniques. Other amino acids did not show any noticeable changes in the emission spectra of 29. However, bovine serum albumin (BSA) triggered

to increase the emission intensity of 29 slightly, but not as strong as those of Cys or Hcys, indicating the difference in their charge and structural motif characters (Figure. 11).

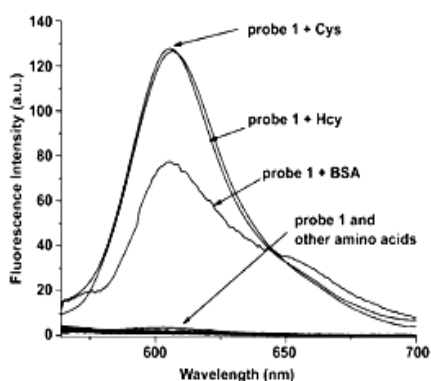
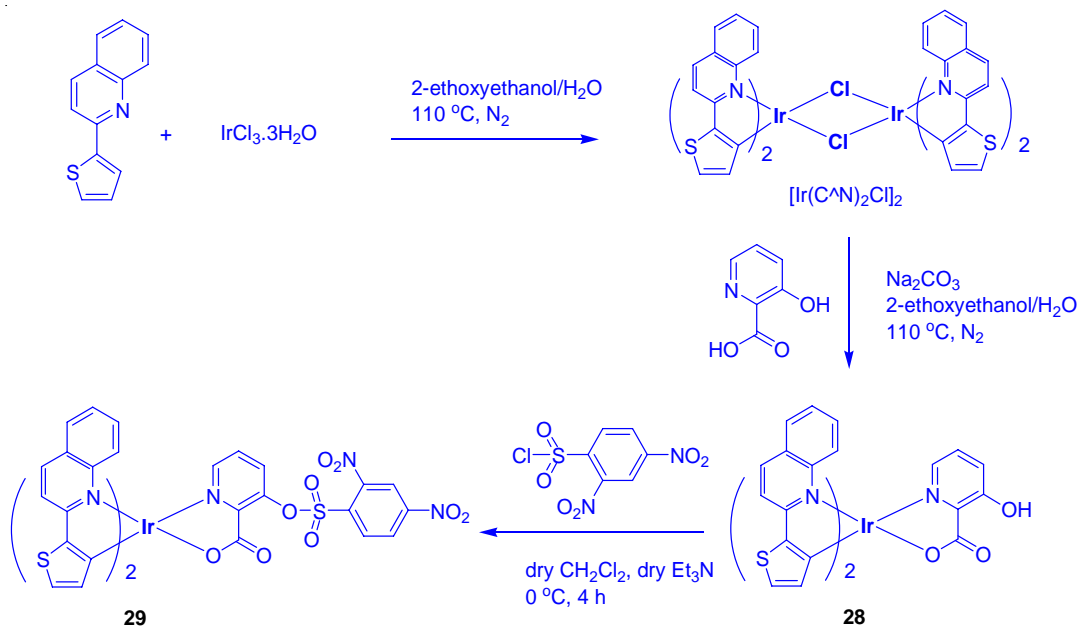


Fig. 11. Emission spectra for probe 29 in the $\text{CH}_3\text{CN}/\text{H}_2\text{O}$ ($8.14 \times 10^{-5} \text{ M}$, 4:1, v/v, pH 7.2) upon addition of various amino acids and proteins (100 equiv). Reproduced with permission from ref. 36. Copyright (2013) John Wiley & Sons

Confocal luminescence imaging studies revealed that probe 29 was able to detect the changes in the concentration of Cys/Hcy in the HeLa living cells (Figure. 12).

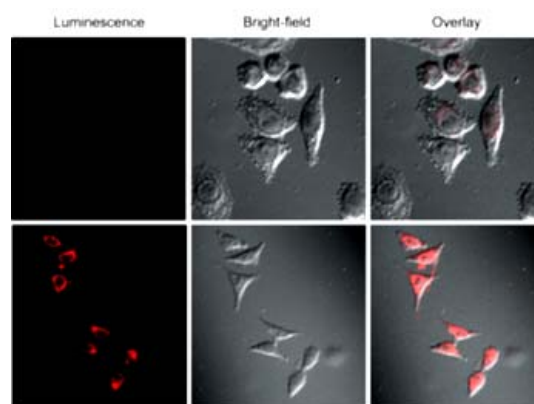
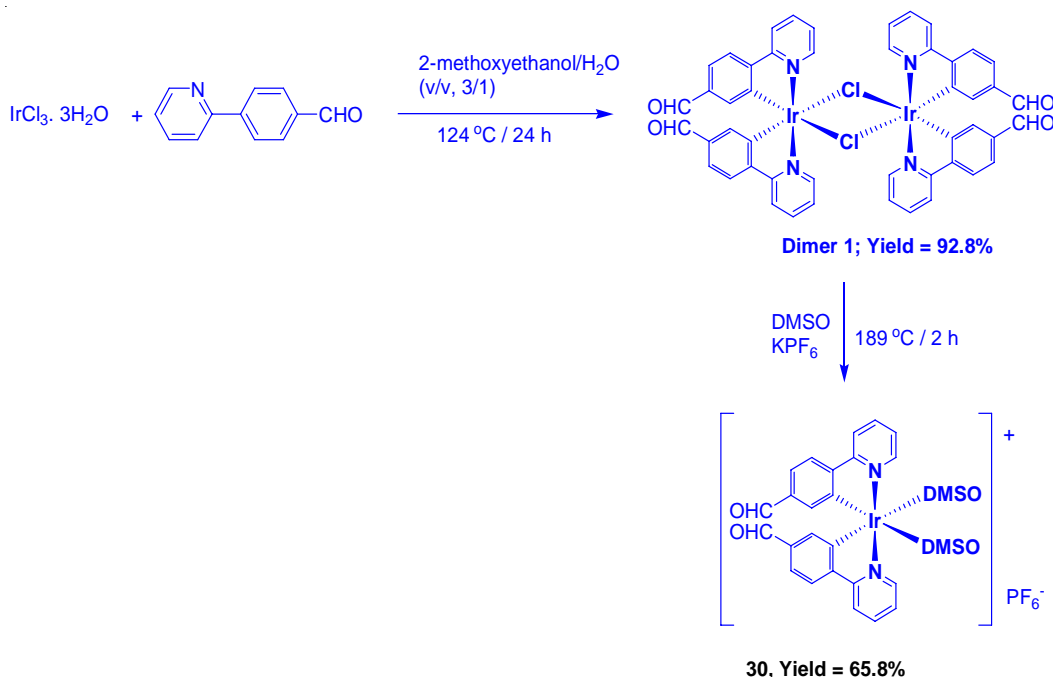


Fig. 12. Luminescence images of probe 29 in HeLa cells. a) HeLa cells incubated with 200 mM N-ethylmaleimide for 30 min and then further incubated with 29 (20 μM) for 30 min. b) HeLa cells incubated with 29 (20 μM) for 30 min. Reproduced with permission from ref. 36. Copyright (2013) John Wiley & Sons

By modulating the structure of iridium complex, Mao and coworkers first studied the

emission glutamine sensing and imaging in live cells³⁷. They prepared an iridium complex containing aldehyde group $[\text{Ir}(\text{pba})_2(\text{DMSO})_2]\text{-PF}_6$ (Hpba = 4-(2-pyridyl)benzaldehyde), (30) by the treatment of

iridium(III) precursor $[(\text{pba})_2\text{Ir}(\mu\text{-Cl})_2\text{Ir}(\text{pba})_2]$, which was obtained by heating the reaction mixture of $\text{IrCl}_3 \cdot 3\text{H}_2\text{O}$ and Hpba, with DMSO in the presence of KPF_6 (Scheme 14).



Scheme 14. Synthesis of cyclometalated iridium(III) complex, 30

Absorption spectrum of 30 exhibited strong absorption bands at 274-324 nm, weak bands at 375-420 nm, and a forbidden band at 650-700 nm, corresponding to the $^1\text{IL}(\pi \rightarrow \pi^*)$ (pba^-), $^1\text{MLCT}$ ($d\pi(\text{Ir}) \rightarrow \pi^*(\text{pba}^-)$) and $^3\text{MLCT}$ ($d\pi(\text{Ir}) \rightarrow \pi^*(\text{pba}^-)$) transitions, respectively. Compound 30 was weakly luminescent at 557 nm with a lifetime of 100 ns, and a quantum yield of 0.04 due to the quenching of emission by electron-withdrawing pba^- moiety, which is supported by DFT calculations. Addition of Glutamine (Gln) into 30 resulted in the decrease of emission intensity at 557 nm initially, but a new peak at 475 nm was generated and increased with a blue shift of 82 nm (Fig. 13). A maximum increase of 200 times in the emission intensity of 30 at 475 nm was registered at 0 to 800 μM of Gln. Other amino acids and Gln-containing peptides did not induce any noticeable changes in the emission spectra of 30. This result demonstrated that complex 30 displayed a high sensitivity and selectivity for Gln. In addition, the DFT calculation and MS spectrometry studies supported the formation of highly emissive 30-Gln complex.

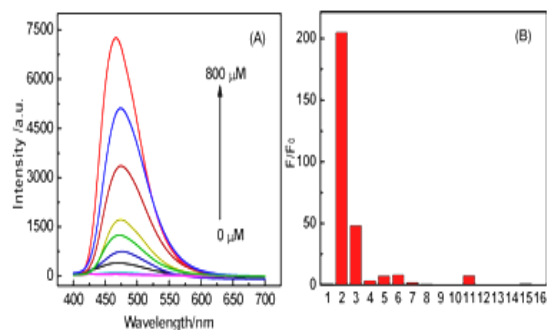


Fig. 13. (A) Emission spectra of 30 solution (10 mM in DMSO/PBS, $v/v = 1/49$) in the presence of increased concentrations of Gln (from bottom to top: 0, 10, 20, 40, 60, 80, 100, 200, 400, 600, and 800 μM); (B) Selective Gln detection using 30. Fluorescence responses (F/F_0) of 30 (10 mM in DMSO/PBS, $v/v = 1/49$) to various amino acids (800 μM) and Gln-containing peptides (800 μM) (from left to right were 1, 30; 2, Gln; 3, Arg; 4, Ala; 5, Asp; 6, Asn; 7, His; 8, Ile; 9, Cys; 10, Tyr; 11, Lys; 12, Gly; 13, Glu; 14, GSH; 15, Ala-Gln; and 16, Gly-Gln. Reproduced with permission from ref. 37. Copyright (2016) American Chemical Society

Complex 30 treated HeLa cells showed a 600-times stronger emission in cytoplasm compared to nucleus. In addition, emission of 30 was further enhanced upon incubation of these cells with Gln (Fig. 14). A high level of co-localization of 30 and mitochondria in which glutamine is an important energy source, was also demonstrated using co-staining with rodamine123. These studies revealed that complex 30 can be a potential platform in studying mitochondrial metabolism.

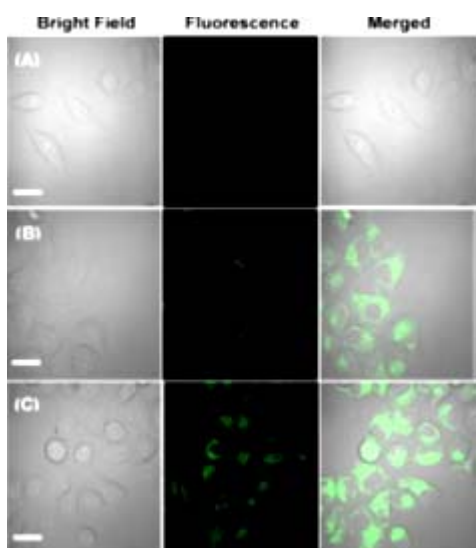
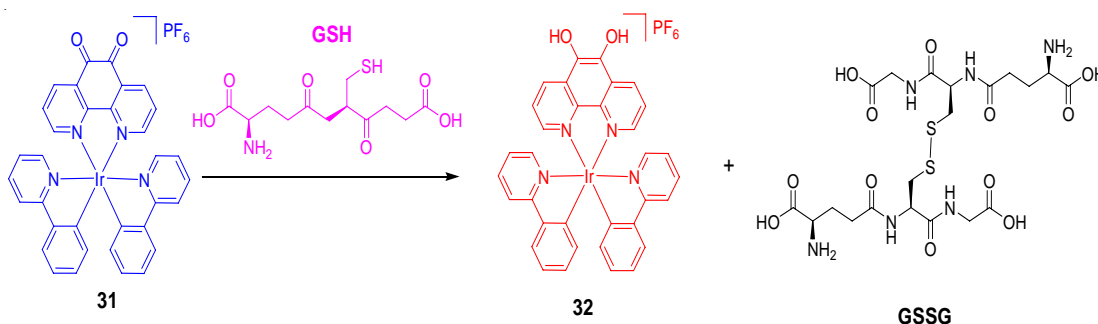


Fig. 14. CLSM and bright-field images of HeLa cells (A) without any treatment; (B) incubated with 20 μM 30 in DMSO/PBS (pH 7.0, 1/49, v/v, 10 mM) for 1 h at 37 $^{\circ}\text{C}$. (C) Pre-incubated with 800 μM Gln for 1 h, then incubated with 20 μM 30 in DMSO/PBS (pH 7.0, 1/49, v/v, 10 mM) for 1 h at 37 $^{\circ}\text{C}$ (λ_{ex} : 405 nm, λ_{em} : 425-470 nm). Scale bar: 20 μm . Reproduced with permission from ref. 37. Copyright (2016) American Chemical Society

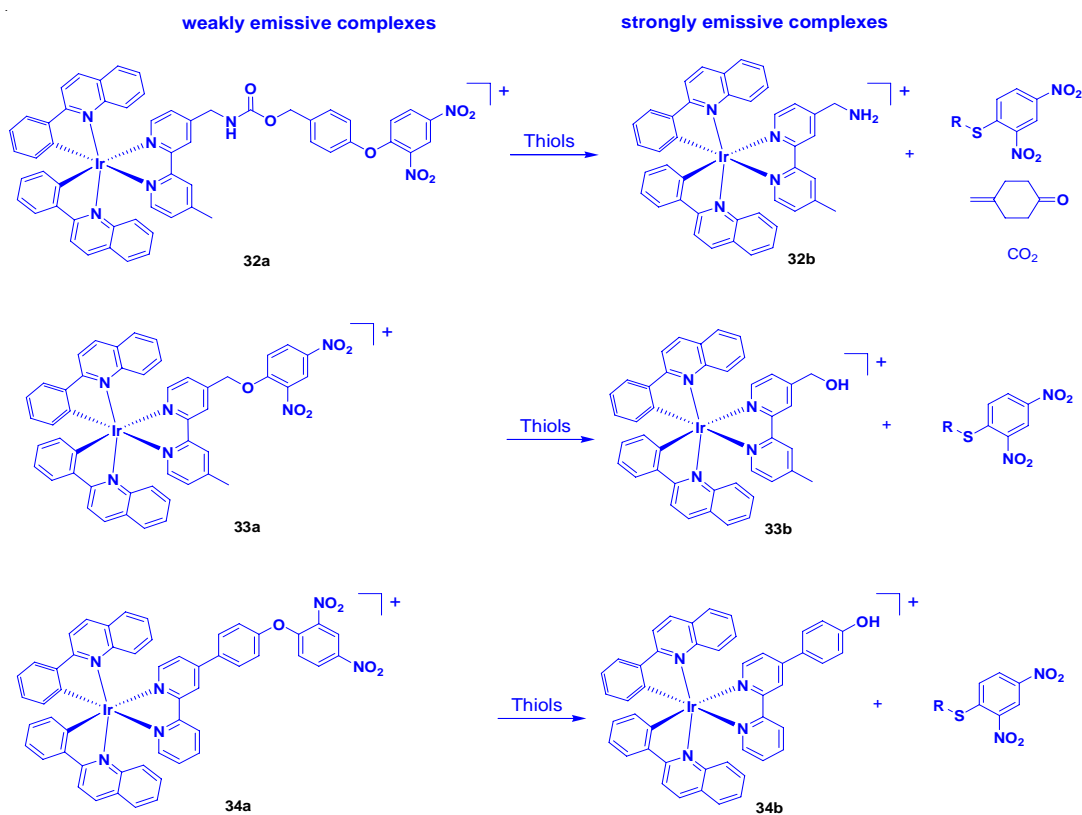
Mao and coworkers³⁸ employed a redox strategy for the detection of thiol amino acid using iridium(III) complex, 31 (Scheme 15). Treatment of $[\text{Ir}(\text{ppy})_2]_2\text{Cl}_2$ (ppy = 2-phenylpyridine) with and 1, 10-phenanthroline-5,6-dione (phendione) in a CH_2Cl_2 :MeOH mixture under reflux condition resulted in the formation of $[\text{Ir}(\text{ppy})_2(\text{phendione})](\text{PF}_6)$ (31). Upon excitation at 350 nm, compound 31 displayed an emission at 587 nm, which is Stokes shifted by 237 nm, with a lifetime of 4.26 μs .

In the absence of GSH, compound 31 exhibited a weak luminescence, but its emission intensity was approximately 3-fold enhanced with a detection limit of 1.67 μM , upon the addition of GSH. Job's plot analysis clearly demonstrated a 1:1 binding stoichiometry of complex 31 with GSH. ^1H NMR and mass spectrometry analyses confirmed that GSH reduced the phendione $\text{N}^{\wedge}\text{N}$ donor in 31 to afford the emissive complex 32 (Scheme 15). Furthermore, the probe 31 was selective for GSH over Cys and other interfering amino acids.

Recently, Lo and coworkers³⁹ prepared three cyclometallated iridium (III) complexes, $[\text{Ir}(\text{pq})_2(\text{N}^{\wedge}\text{N})](\text{PF}_6)$ (32a-34a) (Hpq = 2-phenylquinoline; $\text{N}^{\wedge}\text{N}$ = 4-(N-(4-(2,4-dinitrophenoxy)benzyloxy)carbonyl)aminomethyl-4-methyl-2,2-bipyridine (bpy-dinitro-1) (32a), 4-(2,4-dinitrophenoxy)methyl-4-methyl-2,2-bipyridine (bpy-dinitro-2) (33a), 4-(4-(2,4-dinitrophenoxy)phenyl)-2,2-bipyridine (bpy-dinitro-3) (34)), by the reaction of $[\text{Ir}_2(\text{pq})_4\text{Cl}_2]$ with their corresponding bpy-dinitro derivatives in CH_2Cl_2 /MeOH mixture at room temperature and examined their intracellular thiol sensing ability (Scheme 16).



Scheme 15. Mechanism of GSH detection by iridium(III) complex 31 while GSSG is oxidized by glutathione



Scheme 16. Thiolytic cleavage of complexes 32a-34a leading to the formation of complexes 32b-34b, respectively

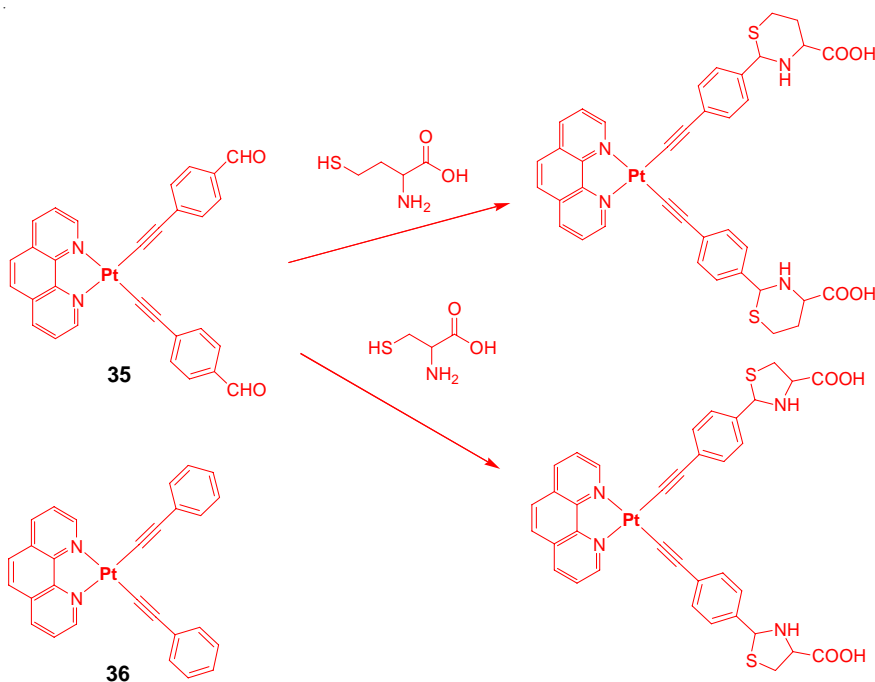
These complexes showed an intraligand ($\pi \rightarrow \pi^*$) (N[^]N and pq) absorption features at 256-309 nm, and ¹MLCT ($d\pi(\text{Ir}) \rightarrow \pi^*(\text{N}^{\wedge}\text{N}$ and pq)) transition at 310-449 nm while their forbidden ³MLCT ($d\pi(\text{Ir}) \rightarrow \pi^*(\text{N}^{\wedge}\text{N}$ and pq)) transition as tailing was observed beyond at 450 nm. Complexes 32a-34a featured a weak emission at 551-555 nm with a shoulder at 588-602 nm in CH₂Cl₂ because of quenching by the dinitrophenyl moiety. Therefore, the observed emission came from ³IL($\pi \rightarrow \pi^*$) (pq) of these complexes. A maximum increase of 2.3-fold in the emission intensity of 32a or 34a was registered upon incubation with GSH or Na₂S (a common source of H₂S) in KPi buffer/MeOH. Whereas compound 33a gave a minimal enhancement because of the presence of shorter linker that might lead to steric effect between thiols and dinitroaromatic moiety. ESI-MS analysis supported the formation of their respective complexes 32b-34b after thiolytic cleavage, confirming that the emission enhancement occurred after leaving the quenching motif.

As these complexes did not respond to biologically relevant RSS (SO₃²⁻, S₂O₃²⁻, and NCS⁻), RNS such as hydrogen peroxide (H₂O₂), peroxide (*t*-BuOOH and O₂⁻), nitrate (NO₃⁻), and nitrite (NO₂⁻), they are considered as good candidates for sensing thiols selectively. When compound 32a was incubated with Na₂S treated HeLa cells, they showed a bright emission in comparison to the cells without pre-treatment of Na₂S. However, a significant weak emission in the cells without pre-treatment of Na₂S was observed due to the presence of endogenous GSH. However, the use of NEM, a common GSH scavenger, made the weakening the emission of complex 32a stained HeLa cells. In another experiment, upon incubation of complex 32a stained HeLa cells with GSH-ester, a bright emissive staining in the cytoplasm region, majority of GSH localized here, was observed. These results demonstrated that complex 32a acted as an effective sensor for GSH and H₂S in living cells.

Platinum(II) complexes

The use of alkynyl-platinum compounds generates highly stable coordination complexes with DNA and amino acids. Huang *et al.*,⁴⁰ prepared two platinum complexes, Pt(phen)(C^oCC₆H₅CHO)₂

(35) and Pt(phen)(C^oCC₆H₅)₂ (36) by the reaction of Pt(phen)Cl₂ and 4-ethynylbenzaldehyde or phenylacetylene, respectively, in the presence of CuI and diethylamine in dichloromethane and used them for cysteine sensing (Scheme 17).



Scheme 17. The chemical structures of compounds 35 and 36 and the probable sensing mechanism of 35 towards Hcy and Cys

Absorption spectra of 35 and 36 displayed several bands below at 400 and a wide band centered at 400 nm, which are ascribed to MLCT and diamine and acetylide-based intra-ligand transitions, respectively. Compound 36 showed an orange emission at 560 nm but compound 35 showed a green emission at 510 nm, which is blue-shifted to 50 nm indicating the presence of electron withdrawing aldehyde group in 35. The addition of Hcys dramatically quenched the emission band of 35 at 510 nm followed by red-shifted to 555 nm along with changing color from green to orange. However, other amino acids did not induce any noticeable changes in the emission spectrum of 35, confirming high selectivity towards Cys/Hcys. Time dependence studies supported that the reaction was complete within 120 min. upon interacting 35 with Cys/Hcys. The selective interaction of 35 with Cys/Hcys was also confirmed by ¹H NMR and DFT analyses. Finally, the authors

concluded that formation of thiazinane led to quenching of 35 along with a red-shifted emission through the reaction of 35 with Cys/Hcys.

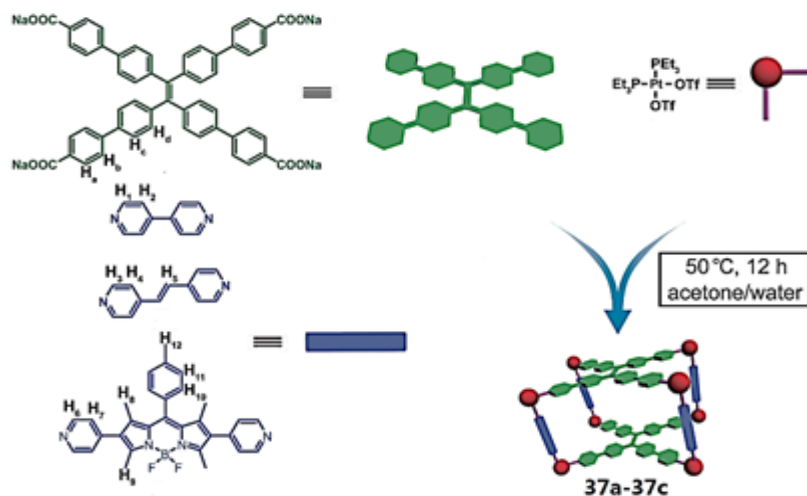
Through a self-destructive mechanism, a turn-on fluorescent sensing of thiol containing amino acids using platinum(II) cage compounds has been reported⁴¹. Three tetragonal prismatic Pt(II) metallacages 37a-37c were prepared by the reaction of Pt(II) acceptors with dipyriddy and tetraphenylethene (TPE)-based sodium benzoate ligands in acetone/water mixture via a metal-coordination driven self-assembly process (Scheme 18). The formation of these cages were confirmed by NMR, ESI-TOF, UV-Vis absorption and fluorescence spectral studies.

In different polar aprotic solvents, cages 37a and 37b showed TPE derivative based absorption bands in the range of 350-370 nm, while

cage 37c displayed BODIPY chromophore based absorption band at 520 nm along with the absorption band of TPE derivative. Cages 37a and 37b exhibited a strong fluorescence at around 493 nm, corresponding to the TPE emission but cage 37c showed two emission peaks at 472 and 544 nm, corresponding the TPE and BODIPY emission, respectively.

Cage 37b was non-emissive in methanol/water mixture. However, the addition of thiol

containing amino acids such as glutathione and cysteine concomitantly increased the intensity of cage 37b at 500 nm with the detection limits in the range of 1.89×10^{-7} and 2.78×10^{-7} M, respectively (Fig. 15). However, other amino acids included glycine, alanine, arginine, lysine, serine, leucine, isoleucine, glutamate, and histidine did not response. This result demonstrated the potential application of cage 37b as a sensor in thiol-containing amino acids.



Scheme 18. Synthetic routes and cartoon representations of cages 37a-37c. Reproduced with permission from ref. 41. Copyright (2017) American Chemical Society

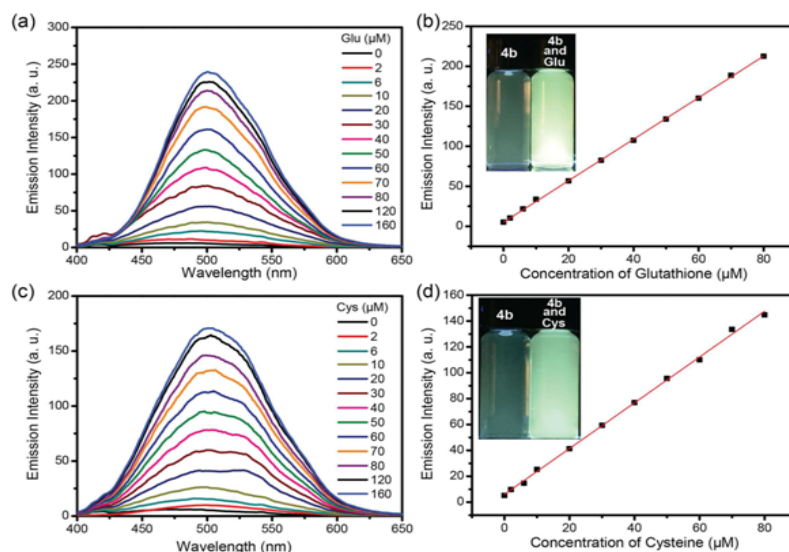
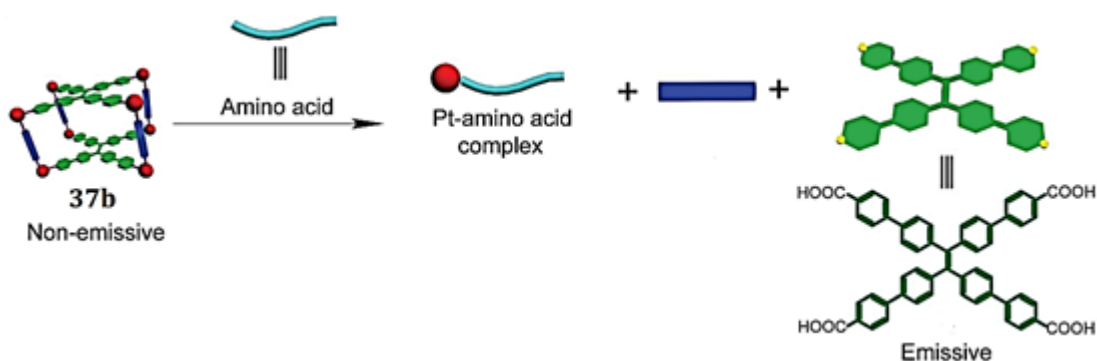


Fig. 15. Fluorescence spectra of cage 37b (10 μM) after 5 min upon the addition of increasing concentrations of glutathione (a) and cysteine (c) and the emission intensities at 500 nm as a function of glutathione (b) and cysteine (d) concentration. Each spectrum was collected in methanol/water (1/1, v/v) with $\lambda_{ex} = 365$ nm. Insets: photographs of 10 μM cage 37b before (left) and after (right) the addition of 160 μM thiol-containing amino acids in methanol/water (1/1, v/v) upon excitation at 365 nm using a UV lamp at 298 K. Reproduced with permission from ref. 41. Copyright (2017) American Chemical Society

^1H NMR titration analysis revealed that thiol amino acids decomposed cage 37b to form mononuclear Pt-amino acid complexes along with benzoic acid derived TPE ligand when cysteine or glutathione was added to a DMSO solution of 37b. $^{31}\text{P}\{^1\text{H}\}$ NMR study confirmed the destruction of 37b upon the addition of these amino acids. A 1:1 binding isotherm was found in the complexation between $\text{Pt}(\text{PEt}_{3/2})(\text{OTf})_2$ and amino acids. Moreover, the regeneration of cage was observed while adding Pt(II) acceptors, indicating the thermodynamic stability of the Pt-amino acid

complexes compared to that of cage. However, cage 37b remained stable even after the addition of 2-mercaptoethanol. This result clearly demonstrated that both thiol and the carboxylic groups performed to function as coordinative ligands with Pt(II) center. As the free TPE derivative was emissive, it functioned as an indicator for the study of thiol-containing amino acids sensing. Based on these results, the authors proposed a self-destructive mechanism for the sensing of Pt(II) caged compounds towards thiol amino acids (Scheme 19).



Scheme 19. Cartoon representation of the self-destructive mechanism. Reproduced with permission from ref. 41. Copyright (2017) American Chemical Society

CONCLUSION

In this review, we have highlighted a series of phosphorogenic heavy metal sensors for the detection of thiol amino acids based on the previously published works. These complexes offer a remarkable structural diversity and tunable emission properties that make them luminescent sensors viable alternatives to organic fluorophores. These probes have been successfully utilized for the sensing and bioimaging of amino acids, especially biothiols, by operating turn-on mechanism via emission enhancement or emission shift (color change) due to electron or energy transfer mechanism. Most of the reported complexes have achieved discrimination between thiol-containing amino acids Cys, Hcys, and GSH, showing excellent selectivity with the lower detection limit. By predicting the interaction of these complexes with thiols, theoretical studies effectively predict to improve the design of structure of metal

complexes. For increasing the solubility of metal complexes, the hydrophilic groups such as quaternary ammonium salt can be incorporated into coordinating ligands of metal complexes and can be used to realize the changes of Cys/Hcys concentration in living cells in aqueous medium.

In spite of significant improvements in this field, several issues that are affected by various factors need to be improved. It would be highly desirable to rationally design phosphorogenic metal complexes with desired properties that can selectively detect and differentiate not only limited to biothiols but also naturally available amino acids. Addition of minimal organic solvent such as CH_3CN and DMSO, because of poor solubility of metal complexes, in bioimaging studies leads to be toxic and destroys the cellular functions, which demerits the application of these metal complexes. Therefore, development of new phosphorogenic heavy metal probes with complete water solubility and higher

selectivity for specific amino acids is an important goal. For bioimaging applications, NIR phosphorogenic heavy metal probes would be highly desirable for the detection of various amino acids in the living cells and tissues because they penetrate very deep with less photodamage and minimum fluorescence background. We envisage that the application of phosphorogenic heavy metal complexes in amino acids sensing will continue to

thrive and mature in this field and will show their commercial applications from research laboratories.

ACKNOWLEDGEMENT

We gratefully acknowledge the financial supports from the Council of Scientific and Industrial Research (CSIR), India and the Academia Sinica, Ministry of Science and Technology, Taiwan.

REFERENCES

- Wood, Z. A., Schroder, E., Harris, J. R., and Poole, L. B., *Trends Biochem. Sci.* **2003**, *28*, 32-40.
- Refsum, H., Smth, A. D., Ueland, P. M., Nexø, E., Clarke, R., Mcpartlin, J., Johnston, C., Engbaek, F., and Schneede, J., *Clin. Chem.* **2004**, *50*, 3-32.
- Shao, N., Jin, J. Y., Cheung, S. M., Yan, R. H., Chan, W. H., and Mo, T., *Angew. Chem. Int. Ed.* **2006**, *45*, 4944-4948.
- Yang, X.-F., Huang, Q., Zhong, Y., Li, Z., Li, H., Lowry, M., Escobedo, J. O., and Strongin, R. M., *Chem. Sci.* **2014**, *5*, 2177-2183.
- Yue, Y., Huo, F., Ning, P., Zhang, Y., Chao, J., Meng, X., and Yin, C., *J. Am. Chem. Soc.* **2017**, *139*, 3181-3185.
- El-Brashy, A. M., and Al-Ghannam, S. M., *Pharm. World Sci.* **1995**, *17*, 54-57.
- Shen, C.-C., Tseng, W.-L., and Hsieh, M.-M. *J. Chromatogr. A* **2009**, *1216*, 288-293.
- Wang, W., Li, L., Liu, S., Ma, C., and Zhang, S., *J. Am. Chem. Soc.* **2008**, *130*, 10846-10847.
- Wang, W., Rusin, O., Xu, X., Kim, K. K., Escobedo, J. O., Fakayode, S. O., Fletcher, K. A., Lowry, M., Schowalter, C. M., Lawrence, C. M., Fronczek, F. R., Warner, I. M., and Strongin, R. M. *J. Am. Chem. Soc.* **2005**, *127*, 15949-15958.
- Sato, Y., Iwata, T., Tokutomi, S., and Kandori, H., *J. Am. Chem. Soc.* **2005**, *127*, 1088-1089.
- Dieckhaus, C. M., Fernández-Metzler, C. L., King, R., Krolkowski, P. H., and Baillie, T. A., *Chem. Res. Toxicol.* **2005**, *18*, 630-638.
- Wang, W., Escobedo, J. O., Lawrence, C. M., and Strongin, R. M., *J. Am. Chem. Soc.* **2004**, *126*, 3400-3401.
- Yang, Y., Zhao, Q., Feng, W., and Li, F. *Chem. Rev.* **2013**, *113*, 192-270.
- Yin, C., Huo, F., Zhang, J., Martinez-Manez, R., Yang, Y., Lv, H., and Li, S., *Chem. Soc. Rev.* **2013**, *42*, 6032-6059.
- Niu, L.-Y.; Chen, Y.-Z.; Zheng, H.-R.; Wu, L.-Z.; Tung, C.-H., and Yang, Q.-Z. *Chem. Soc. Rev.* **2015**, *44*, 6143-6160.
- Wang, J., Liu, H.-B., Tong, Z., and Ha, C.-S., *Coord. Chem. Rev.* **2015**, *303*, 139-184.
- Ma, D.-L., Ma, V. P.-Y., Chan, D. S.-H., Leung, K.-H., He, H.-Z., and Leung, C.-H., *Coord. Chem. Rev.* **2012**, *256*, 3087-3113.
- Zhao, Q., Li, F., and Huang, C., *Chem. Soc. Rev.* **2010**, *39*, 3007-3030.
- Lo, K. K. W., Hui, W. K., Ng, D. C. M., and Cheung, K. K., *Inorg. Chem.* **2002**, *41*, 40-46.
- Amoroso, A. J., Arthur, R. J., Coogan, M. P., Court, J. B., Fernandez-Moreira, V., Hayes, A. J., Lloyd, D., Millet, C., and Pope, S. J. A., *New J. Chem.* **2008**, *32*, 1097-1102.
- Weh, J., Duerkop, A., and Wolfbein, O. S., *ChemBioChem.* **2007**, *8*, 122-128.
- Ji, S., Guo, H., Yuan, X., Li, X., Ding, H., Gao, P., Zhao, C., Wu, W., Wu, W., and Zhao, J., *Org. Lett.* **2010**, *12*, 2876-2879.
- Zhang, R., Yu, X., Ye, Z., Wang, G., Zhang, W., and Yuan, J., *Inorg. Chem.* **2010**, *49*, 7898-7903.
- Li, M.-J., Zhan, C.-Q., Nie, M.-J., Chen, G.-N., and Chen, X., *J. Inorg. Biochem.* **2011**, *105*, 420-425.
- Zhang, W., Zhang, R., Zhang, J., Ye, Z., Jin, D., and Yuan, J., *Anal. Chim. Acta*, **2012**, *740*, 80-87.
- Zhang, R., Ye, Z. Q., Yin, Y. J., Wang, G. L., Jin, D. Y., Yuan, J. L., and Piper, J. A., *Bioconjugate Chem.* **2012**, *23*, 725-733.
- Li, G.-Y., Liu, J.-P., Huang, H.-Y., Wen, Y.,

- Chao, H., and Ji, L.-N., *J. Inorg. Biochem.* **2013**, *121*, 108-113.
28. Ye, Z., Gao, Q., An, X., Song, B., and Yuan, J., *Dalton Trans.* **2015**, *44*, 8278-8283.
29. Ma, D.-L., Wong, W.-L., Chung, W.-H., Chan, F.-Y., So, P.-K., Lai, T.-S., Zhou, Z.-Y., Leung, Y.-C., and Wong, K.-Y., *Angew. Chem. Int. Ed.* **2008**, *47*, 3735-3739.
30. Zhao, N., Wu, Y.-H., Shi, L.-X., Lin, Q.-P., and Chen, Z.-N., *Dalton Trans.* **2010**, *39*, 8288-8295.
31. Chen, H. L., Zhao, Q., Wu, Y. B., Li, F. Y., Yang, H., Yi, T., and Huang, C. H., *Inorg. Chem.* **2007**, *46*, 11075-11081.
32. Xiong, L., Zhao, Q., Chen, H., Wu, Y., Dong, Z., Zhou, Z., and Li, F., *Inorg. Chem.* **2010**, *49*, 6402-6408.
33. Shiu, H.-Y., Wong, M.-K., and Che, C.-M., *Chem. Commun.* **2011**, *47*, 4367-4369.
34. Ma, Y., Liu, S., Yang, H., Wu, Y., Yang, C., Liu, X., Zhao, Q., Wu, H., Liang, J., Li, F., and Huang, W., *J. Mater. Chem.* **2011**, *21*, 18974-18982.
35. Li, C., Yu, M., Sun, Y., Wu, Y., Huang, C., and Li, F., *J. Am. Chem. Soc.* **2011**, *133*, 11231-11239.
36. Tang, Y., Yang, H.-R., Sun, H.-B., Liu, S.-J., Wang, J.-X., Zhao, Q., Liu, X.-M., Xu, W.-J., Li, S.-B., and Huang, W., *Chem. Eur. J.* **2013**, *19*, 1311-1319.
37. Jiang, Q., Wang, M., Yang, L., Chen, H., and Mao, L., *Anal. Chem.* **2016**, *88*, 10322-10327.
38. Mao, Z., Liu, J., Kang, T.-S., Wang, W., Han, Q.-B., Wang, C.-M., Leung, C.-H., and Ma, D.-L., *Sci. Technol. Adv. Mater.* **2016**, *17*, 110-114.
39. Tso, K. K.-S., Liu, H.-W., and Lo, K.K.-W., *J. Inorg. Biochem.* **2017**, *177*, 412-422.
40. Huang, K., Yang, H., Zhou, Z., Chen, H., Li, F., Yi, T., and Huang, C., *Inorg. Chim. Acta* **2009**, *362*, 2577-2580.
41. Zhang, M., Saha, M. L., Wang, M., Zhou, Z., Song, B., Lu, C., Yan, X., Li, X., Huang, F., Yin, S., and Stang, P. J., *J. Am. Chem. Soc.* **2017**, *139*, 5067-5074.